STRUCTURAL BIOLOGY

Mitoribosomal small subunit biogenesis in trypanosomes involves an extensive assembly machinery

Martin Saurer[1]*, David J. F. Ramrath[1]*, Moritz Niemann[2]*, Salvatore Calderaro[2], Céline Prange[1], Simone Mattei[1], Alain Scaiola[1], Alexander Leitner[3], Philipp Bieri[1], Elke K. Horn[2], Marc Leibundgut[1], Daniel Boehringer[1], André Schneider[2]†, Nenad Ban[1]†

Mitochondrial ribosomes (mitoribosomes) are large ribonucleoprotein complexes that synthesize proteins encoded by the mitochondrial genome. An extensive cellular machinery responsible for ribosome assembly has been described only for eukaryotic cytosolic ribosomes. Here we report that the assembly of the small mitoribosomal subunit in *Trypanosoma brucei* involves a large number of factors and proceeds through the formation of assembly intermediates, which we analyzed by using cryo–electron microscopy. One of them is a 4-megadalton complex, referred to as the small subunit assemblosome, in which we identified 34 factors that interact with immature ribosomal RNA (rRNA) and recognize its functionally important regions. The assembly proceeds through large-scale conformational changes in rRNA coupled with successive incorporation of mitoribosomal proteins, providing an example for the complexity of the ribosomal assembly process in mitochondria.

Although they share a common ancestor, mitochondrial ribosomes (mitoribosomes) are substantially different in composition and structure from bacterial ribosomes, with an increased number of proteins and ribosomal RNA (rRNA) that varies considerably in length (*1*). An extreme example of a mitoribosome with an unusually large number of proteins and highly reduced rRNAs is found in *Trypanosoma brucei*, a parasitic protozoan that causes sleeping sickness in humans (*2*). Due to the complexity of mitoribosomes, it is conceivable that a dedicated machinery comprising assembly factors evolved for mitoribosomal maturation. Ribosome biogenesis is a multistep process in which rRNA folds, often cotranscriptionally, and ribosomal proteins are recruited (*3*–*5*). Assembly and maturation of eukaryotic cytosolic ribosomes are facilitated by numerous factors that form large complexes together with ribosomal proteins and immature rRNA (*5*). For mitoribosomes, structures of mammalian late assembly intermediates of the large subunit (LSU), to which three assembly factors are bound, have been described (*6*). Although it has been suggested that some proteins detected in purified mitoribosomal small subunits (mt-SSUs) from *T. brucei* may be involved in mitoribosomal maturation (*7*) and several mitochondrial assembly factors in yeast and human have been described, it is not clear whether mitoribosomal assembly involves formation of large assembly complexes, and there is currently no structural information that would provide a more comprehensive overview of mitoribosomal biogenesis in any organism.

To better understand mitoribosome biogenesis, we analyzed three assembly intermediates of the mt-SSU from *T. brucei* by using single-particle cryo–electron microscopy (cryo-EM). We were able to determine the atomic structure of the earliest and largest of the analyzed intermediates, which we termed the mt-SSU assemblosome, and this allowed us to identify 34 assembly factors that participate in the maturation of the trypanosomal mt-SSU. Comparison of the assemblosome with the two other assembly intermediates and the mature trypanosomal mt-SSU (*2*), together with RNA interference (RNAi) experiments for selected assembly factors, provides insights into the complex mechanisms of mitoribosomal assembly.

Assembly intermediates of the trypanosomal mt-SSU

T. brucei mitoribosomal particles were purified from a native mitochondrial sample by using sucrose gradient fractionation (see the supplementary materials). We used cryo-EM to analyze the sample and noticed several mt-SSU–related particles with varied abundance levels (Figs. 1 and 2). From these particles, we were able to calculate structures of three complexes, which reached medium resolutions (fig. S1). To enrich the largest of the complexes during purification, we used a PTP tag (*8*) on the ribosomal protein uS17m, which allowed us to considerably improve the overall resolution of the reconstruction to 3.3 Å and to 3.1 Å when we accounted for independent movement of domains (Fig. 1A and figs. S2 and S3).

The structure of the largest assembly revealed the 620-nucleotide 9*S* rRNA in an immature state (Fig. 3) and 43 out of the 55 ribosomal proteins of the trypanosomal mt-SSU (*2*), along with 34 additional, nonribosomal proteins. The combined molecular mass of all identified proteins in this complex is ~4 MDa. Several of the nonribosomal proteins are structural homologs of known ribosome assembly factors from bacteria and mitochondria, such as methyltransferases and pseudouridine synthases, that stabilize and modify the rRNA during ribosome assembly. We used RNAi to knock down seven of these proteins in *T. brucei* cells and observed a specific reduction of the 9*S* rRNA in all cases (Fig. 4 and fig. S4), indicating a critical importance of these factors for rRNA stability, as observed for mitoribosomal assembly factors of other species (*9*). Furthermore, we noticed reduced growth rates of cell cultures, implying that the knockdowns hampered mitochondrial translation by reducing the amounts of functional mt-SSUs. These findings provided evidence that the nonribosomal proteins are assembly factors and that the 4-MDa complex is an assembly intermediate of the mt-SSU.

The reconstructions of the two other mt-SSU–related complexes were resolved to 5.2 and 6.1 Å, respectively (fig. S5). We determined their architecture and composition by comparison with the 4-MDa assembly intermediate and the mature mt-SSU (*2*). The results indicated that we were likely observing further intermediates of the mitoribosomal assembly process, because the first of the two complexes contained 14 of the 34 assembly factors and two additional ribosomal proteins, whereas the second complex contained the complete set of 55 ribosomal proteins with two of the assembly factors remaining (Fig. 2). The intersubunit sides of both additional complexes are covered by large unassigned densities with recognizable protein secondary structure elements, possibly corresponding to additional assembly factors that join later during the assembly.

Here, we refer to the 4-MDa complex as the mt-SSU assemblosome, to the nonribosomal proteins as mt-SSU assembly factors (mt-SAFs) (fig. S6 and table S2), and to the first and second additional complexes as middle and late assembly intermediates. Nevertheless, our results provide neither an indication for the kinetics of the assembly process nor distinction between on- and off-pathway assembly intermediates.

Structure of the mt-SSU assemblosome

Due to the presence of a large number of assembly factors, the shape of the mt-SSU assemblosome is considerably different from that of the mature mt-SSU (Figs. 1 and 2). A visually striking, tower-like protrusion that emerges from the intersubunit side of the assemblosome is formed by the homopentameric assembly factor mt-SAF24. The head of the assemblosome contains all ribosomal proteins of the mature head but is distorted,

[1]Department of Biology, Institute of Molecular Biology and Biophysics, ETH Zurich, Otto-Stern-Weg 5, CH-8093 Zurich, Switzerland. [2]Department of Chemistry and Biochemistry, University of Bern, Freiestrasse 3, CH-3012 Bern, Switzerland. [3]Department of Biology, Institute of Molecular Systems Biology, Otto-Stern-Weg 3, ETH Zurich, CH-8093 Zurich, Switzerland.
*These authors contributed equally to this work.
†Corresponding author. Email: andre.schneider@dcb.unibe.ch (A.S.); ban@mol.biol.ethz.ch (N.B.)

as a cluster of assembly factors is inserted as a wedge between the head and the assembly factors of the body at the entry of the immature mRNA channel. The protein composition of the body is less complete, lacking 12 ribosomal proteins (uS12m, bS21m, mS37, mS42, mS43, mS47, mS48, mS60, mS61, mS64, mS66, and mS74). Large parts of the body, where ribosomal proteins are missing, are covered by assembly factors that interact with ribosomal proteins and rRNA.

The immature, A- and U-rich 9*S* rRNA of the assemblosome (Fig. 3A) contains only a few stabilizing base pairs, similar to the 9*S* rRNA of the mature mt-SSU (*2*). Whereas some regions of the rRNA are well ordered and stabilized

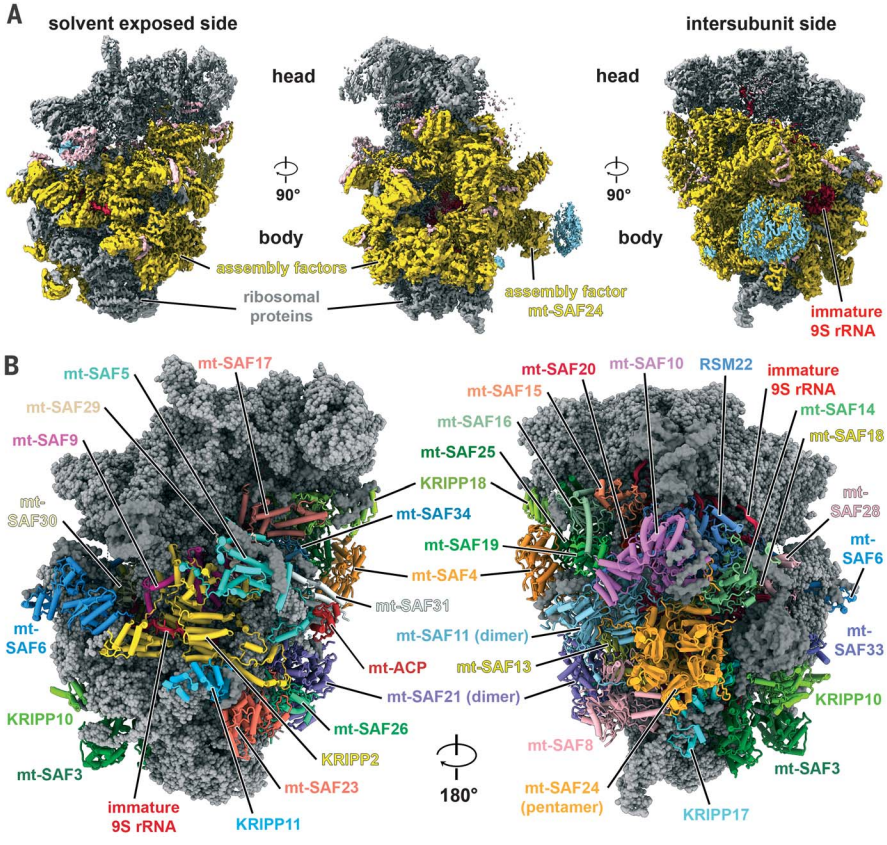

Fig. 1. The structure of the trypanosomal mt-SSU assemblosome. (**A**) The cryo-EM reconstruction shows density for ribosomal proteins (gray), assembly factors (yellow), rRNA (red), and unidentified proteins (pink). Some densities could not be assigned to protein or rRNA (light blue); this is most apparent on the top of the homopentameric assembly factor mt-SAF24. (**B**) Atomic model of the assemblosome with ribosomal proteins (gray) and individually colored assembly factors. Unidentified proteins are shown as gray surface models.

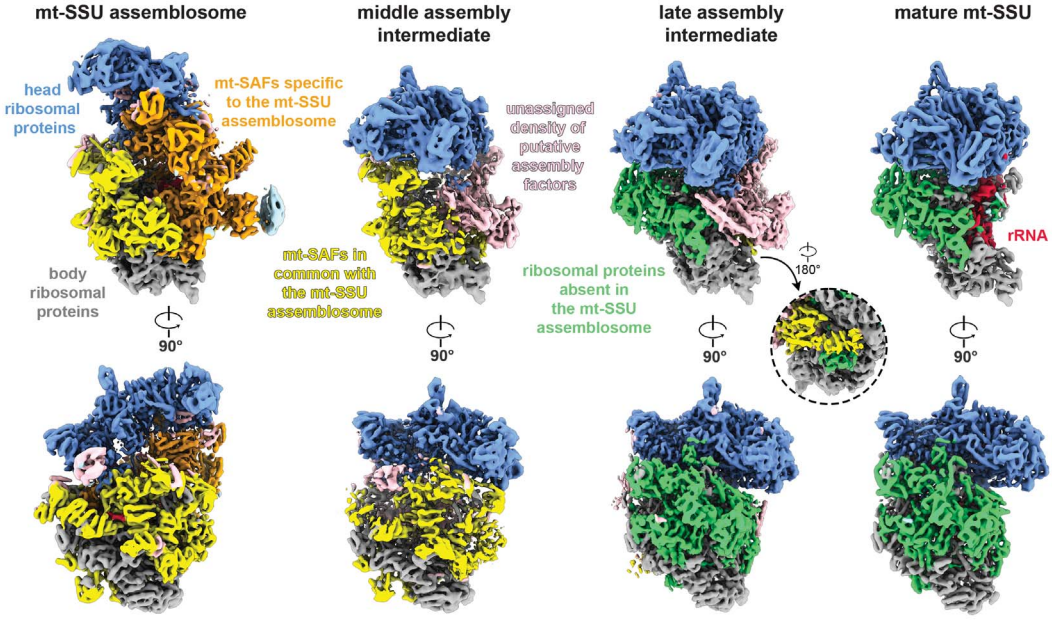

Fig. 2. Comparison of the assembly intermediates and the mature trypanosomal mt-SSU. Reconstructions of the assembly intermediates and the mature mt-SSU are shown filtered to 6-Å resolution. The assembly factors located at the solvent-exposed side of the assemblosome (yellow) are also found on the middle and in part on the late assembly intermediate. Most assembly factors at the intersubunit side of the assemblosome are specific to this complex (orange). The structures of later assembly intermediates feature densities for other putative assembly factors (pink) at locations that were previously occupied by assemblosome-specific factors. In the late assembly intermediate, ribosomal proteins that are not present on the assemblosome (green) replace most assembly factors.

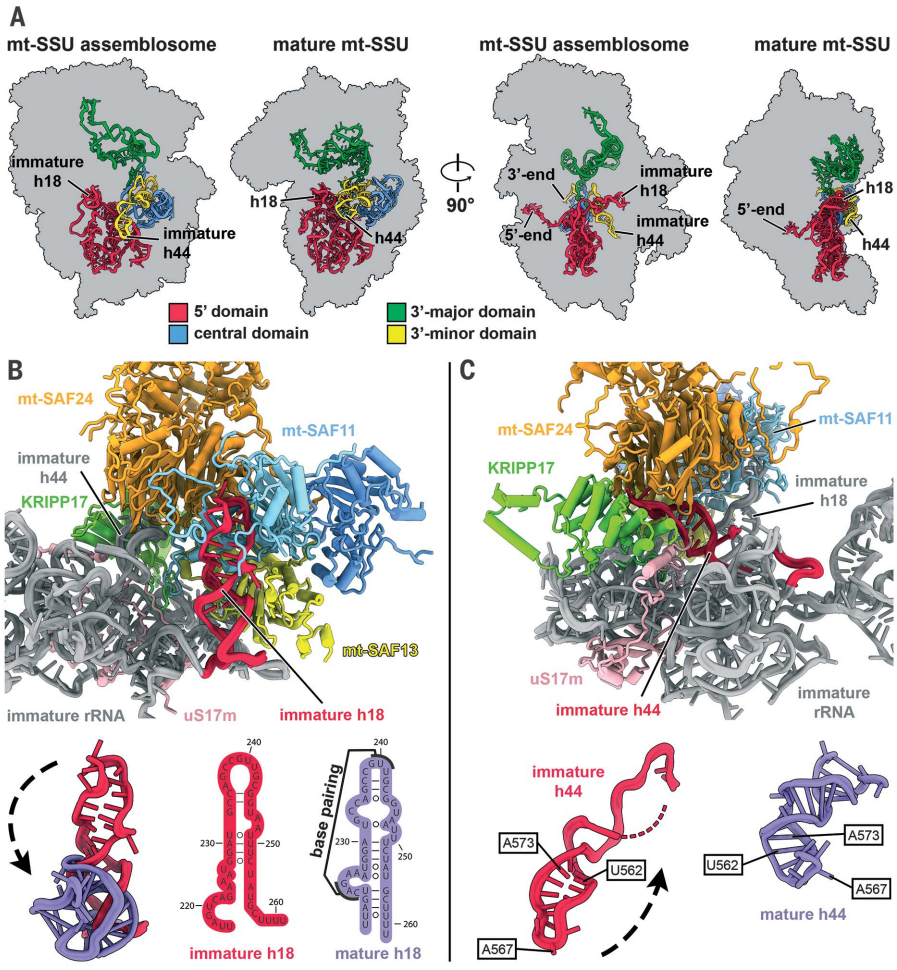

Fig. 3. Features of the immature 9S rRNA of the mt-SSU assemblosome. (**A**) Comparisons of the immature and mature 9S rRNA, shown in the same orientation. Notably, the 3′ major domain, helices h18 and h44, and the 5′ and 3′ ends differ substantially in the two complexes. Nucleotides of uncertain orientation are shown only as backbone. (**B**) The homodimeric pseudouridine synthase mt-SAF11 (subunits in shades of blue) is located on top of the methyltransferase-like assembly factor mt-SAF13 (yellow) and encompasses the immature h18 (red). Maturation of h18 requires a rotation and refolding to form the pseudoknot structure of mature h18 (purple). (**C**) The immature h44 (red) is held in place by the assembly factors KRIPP17 (green) and mt-SAF24 (orange), which interact with both immature helices h18 and h44. Maturation of h44 includes a rotation and retraction as well as a shift in base pairings.

by interactions with ribosomal proteins and assembly factors, other parts are more flexible due to the absence of interacting proteins (fig. S7, A and B). Thus, nucleotides 542 to 553 could not be modeled. As the rRNA matures, the entire 3′-major domain of the rRNA moves considerably relative to the other rRNA domains. Furthermore, local conformational changes and intricate reorganizations must occur along the entire rRNA, such as refolding, establishment of alternative base pairing, and shifting of rRNA strands (Fig. 3, B and C, and fig. S7C).

The incomplete set of ribosomal proteins and the partially immature rRNA indicate that the mt-SSU assemblosome represents an early to middle stage of assembly. This is supported by the absence of two ribosomal proteins, uS12m and bS21m, whose bacterial orthologs have been described to bind to the SSU at a late stage of assembly (*10*). Additionally, the rotated head resembles in vitro–reconstituted assembly intermediates of the bacterial SSU that also lack uS12 and bS21 (*11*).

The middle assembly intermediate retained 14 assembly factors of the assemblosome [KRIPP2 (mt-SAF2), mt-SAF3, mt-SAF5, mt-SAF6, KRIPP10 (mt-SAF7), mt-SAF9, mt-SAF21, KRIPP17 (mt-SAF22), mt-SAF23, mt-SAF26, KRIPP11 (mt-SAF27), mt-SAF29, mt-SAF31, and mt-ACP (mt-SAF32)], which are located primarily on the solvent-exposed side. Compared with the assemblosome, the middle assembly intermediate contains two additional ribosomal proteins (uS12m and mS74). The late assembly intermediate is the most mature of the three complexes, containing all ribosomal proteins of the mt-SSU and only two assembly factors of the assemblosome (KRIPP10 and KRIPP17). The wedge-shaped assembly factor cluster between the head and the body of the assemblosome is absent on the middle and late assembly intermediates and, consequently, the head is shifted to its mature position. Furthermore, most assembly factors at the intersubunit side are absent and seem to be replaced by other, still-uncharacterized factors.

Conformations of the decoding center-forming rRNA helices

In the mature mt-SSU, the rRNA helices h18 and h44 are part of the decoding center and play critical roles during translation. In the assemblosome, h18 is kept in an immature, stretched-out conformation by the homodimeric assembly factor mt-SAF11, which contains a pseudouridine synthase fold (Fig. 3B). In bacteria, h18 of the 16*S* rRNA is modified by the pseudouridine synthase RsuA, which introduces a pseudouridine at U516 (*Escherichia coli* numbering) (*12*, *13*). It is possible that in trypanosomal mitochondria mt-SAF11 has the same function as RsuA in bacteria; however, the exact target uridine could not be identified. To fold into the characteristic pseudoknot observed in the structure of the mature subunit (*2*), h18 has to rearrange its base-pairing pattern, rotate, and move up to 60 Å. This transformation might occur together with the incorporation of uS12m during the transition from the assemblosome to the middle assembly intermediate, as this ribosomal protein interacts with the non-extended h18 present in the middle and late assembly intermediates.

As observed for h18, helix h44 adopts an extended conformation in the assemblosome. mt-SAF22, which is also termed kinetoplast ribosomal pentatricopeptide repeat (PPR)-containing protein 17 (KRIPP17) (*14*), and two subunits of mt-SAF24 bind to h44 from opposite sides and stabilize the immature state (Fig. 3C). The transformation of h44 into the mature conformation includes a rotation, a shift in the base-pairing pattern, and a retraction of ~30 Å and likely

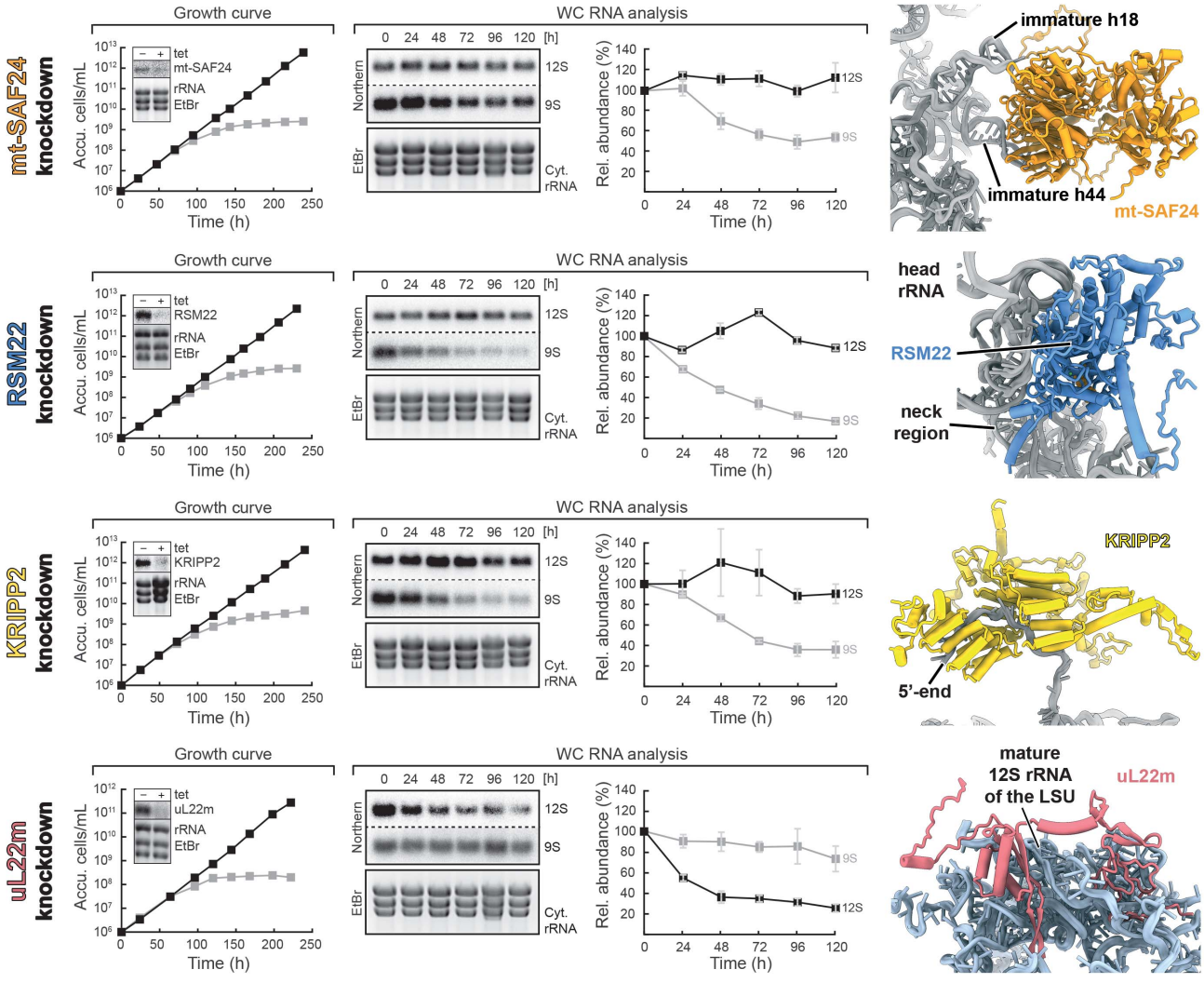

Fig. 4. Importance of assembly factors for cell growth and rRNA stability. The protein levels of the assembly factors mt-SAF24, RSM22, and KRIPP2 were reduced by tetracycline (tet)–inducible RNAi in *T. brucei* cells. The knockdown of uL22m, a ribosomal protein of the large subunit, served as a control. Accumulated cell counts show that all knockdown cultures experienced a stall in growth after induction. The levels of 12*S* and 9*S* rRNA in induced knockdown strains were determined at 24-hour intervals via Northern blotting. Whole-cell (WC) RNA analysis of mt-SAF knockdown cultures showed specific reduction in the 9*S* rRNA levels, likely caused by the loss of structural integrity and subsequent degradation of the 9*S* rRNA. The levels of 12*S* rRNA and the cytosolic rRNAs remained unaffected. uL22m knockdown cultures exhibited the opposite effect, showing reduced 12*S* and relatively constant 9*S* rRNA levels. The structures of the analyzed proteins are shown together with their corresponding rRNA interaction sites. Cultures were grown in triplicates. Cytosolic rRNA bands were visualized by ethidium bromide staining as a loading control. Error bars indicate the average deviations from the means.

takes place after the assemblosome and before the middle assembly intermediate state.

Structures and functions of assembly factors

In the assemblosome, we observed four assembly factors with homology to class I methyltransferases, enzymes that methylate rRNA to promote maturation, fine-tune ribosomal function, and provide resistance to antibiotics (*15*, *16*). RSM22 (mt-SAF1) (*17*), mt-SAF13, and mt-SAF14 form extensive interactions with the immature rRNA, whereas mt-SAF4 does not contact rRNA (fig. S8, A and B). For RSM22 and mt-SAF14, we observed density in the catalytic center likely corresponding to the cofactor *S*-adenosylmethionine or *S*-adenosylhomocysteine. RSM22 is the largest assembly factor of the assemblosome and essential for 9*S* rRNA maintenance (Fig. 4). It contains a zinc finger domain and is homologous to yeast RSM22 and human methyltransferase-like protein 17 (METTL17) (fig. S8C) (*18*). mt-SAF13 is located close to h18, which contains a well-conserved sequence at its apical loop. In bacteria, the methyltransferase RsmG methylates G527 (*E. coli* numbering) in the apical loop of h18 (*16*). In the trypanosomal mt-SSU assemblosome, the corresponding G242 would be able to reach into the active site of mt-SAF13 upon a modest conformational change of the immature, extended h18 (fig. S8D). Thus, mt-SAF13 might act as an RsmG homolog that introduces a methyl group at this conserved position. mt-SAF14 resembles bacterial RsmH, which is responsible for methylation of C1402 (*E. coli* numbering) in h44 during bacterial SSU maturation (*19*, *20*). mt-SAF14 is located next to RSM22, close to h44 and h45, suggesting that it methylates a nucleotide of the 3′-domain (fig. S8E). However, for any of the trypanosomal methyltransferases, further research is required to determine their target nucleotides.

Five of the 34 identified assembly factors belong to the KRIPP family (*14*, *21*) (fig. S6 and table S2). Only KRIPP2 and KRIPP10 are large enough to form extended superhelical spiral structures, and

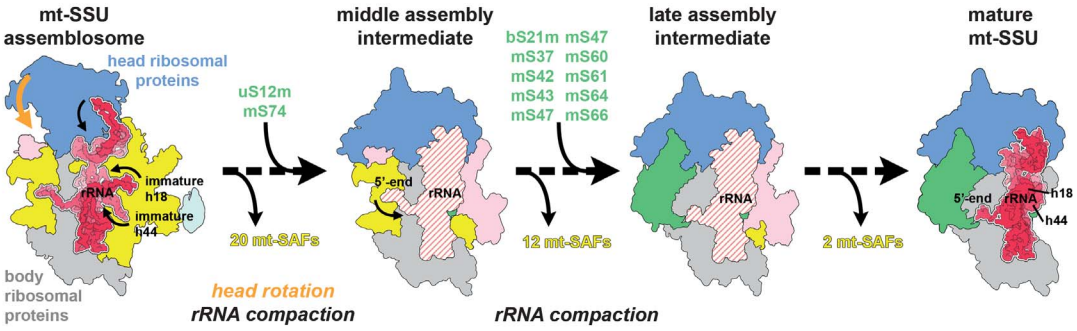

Fig. 5. Summary of maturation processes from the assemblosome to the mature mt-SSU. The immature 9S rRNA of the mt-SSU assemblosome is stabilized between the ribosomal proteins of the body (gray) or the head (blue) and the bound assembly factors (yellow). Stepwise dissociation of the assembly factors allows the head to rotate into the mature conformation (orange arrow), whereas the rRNA (red, or red striped for tentatively fitted rRNA segments) undergoes compaction by retraction of the extensions (black arrows) such as the 5′-end, h18, and h44, which are released from the assembly intermediates. In parallel, the 12 missing ribosomal proteins associate to form the complete, mature mt-SSU. The likely existence of unknown transition states between the observed assembly intermediates and the possibility of parallel assembly pathways are indicated by dashed arrows.

only KRIPP2 wraps around single-stranded RNA in a prototypical manner (*22*, *23*), specifically recognizing the 5′-end region of the 9*S* rRNA and cradling the rRNA with its positively charged interaction surface (fig. S9). All other KRIPPs contact rRNA differently or not at all, which indicates that KRIPPs fulfill a variety of functions by binding to other ribosomal proteins, assembly factors, or rRNA. Additionally, our structure shows that KRIPPs not only are part of the mature ribosome but also act as ribosome assembly factors. The importance of this role is exemplified by the destabilization of 9*S* rRNA in KRIPP2 and KRIPP17 knockdown experiments (Fig. 4 and fig. S4). Furthermore, with its binding site at the 5′-end, KRIPP2 might be one of the first proteins that associate with the newly transcribed rRNA.

In the assemblosome, a wedge-shaped cluster is formed by nine assembly factors [mt-SAF4, KRIPP18 (mt-SAF12), mt-SAF15, mt-SAF17, mt-SAF20, mt-SAF34, and a heterotrimer consisting of mt-SAF16, mt-SAF19, and mt-SAF25] and the ribosomal protein uS3m (fig. S10). The highly hydrophobic uS3m is one of only two ribosomal proteins encoded in the trypanosomal mitochondrial genome (*2*). uS3m is anchored to the ribosomal proteins of the head domain via its long N-terminal tail, whereas the folded, hydrophobic C-terminal domain forms a β sheet with mt-SAF17 and mt-SAF34 (fig. S11, A and B). The C-terminal domain of uS3m interacts almost exclusively with assembly factors and, therefore, has to be handed over to establish interactions with ribosomal proteins in the mature subunit (fig. S11, C and D). Based on the hydrophobic character of uS3m, surrounding assembly factors likely assume a chaperoning role to deliver uS3m to the immature SSU; this interaction is analogous to that for uS3 of eukaryotic cytosolic ribosomes and its ankyrin repeat chaperone, Yar1 (*24*, *25*).

In addition to the above-discussed mt-SAFs, we observed assembly factors with folds homologous to those of a metallo-β-lactamase (mt-SAF20), an ADP-ribosyl-glycohydrolase (mt-SAF23), a BTB domain (mt-SAF24) (fig. S12), a tyrosine phosphatase (mt-SAF26), and LYR motif proteins (mt-SAF31) bound to an acylated mt-ACP (mt-SAF32). The latter two proteins have been suggested to link fatty acid synthesis to the assembly of the mt-LSU and of the electron transport chain (*6*, *26*).

Large-scale conformational changes of ribosomal proteins during maturation

Considering that ribosomal proteins of the trypanosomal mt-SSU, unlike ribosomal proteins in bacteria, form extensive interactions, early binding proteins often have to change conformation to accommodate the later binding proteins. These maturation-dependent conformational changes are widespread and observed in both conserved and trypanosoma-specific ribosomal proteins (fig. S13). We observed that during maturation the core domains of conserved ribosomal proteins such as uS5m, bS6m, uS8m, and uS15m barely move, whereas their trypanosome-specific N- and C-terminal extensions are heavily remodeled. For trypanosome-specific ribosomal proteins such as mS68, the structural changes can also affect the core domains. The conformational changes in ribosomal proteins affect maturation processes through various means, such as by blocking binding sites of late associating ribosomal proteins in the case of mS68 or by stabilizing the 9*S* rRNA in its immature conformation, as seen for mS59.

Folding flexible rRNA into a protein shell

In addition to conformational changes of individual proteins, movements of protein clusters as rigid blocks are necessary for mt-SSU maturation. For instance, the ribosomal proteins of the head have to move as two rigid blocks toward the body (fig. S14). The rRNA, although linked to these blocks at several positions, is flexible and has to refold to attain the mature conformation, often by shifting single rRNA strands. At the 5′-end or in the h23 region, rRNA has to shift across a rigid protein interface provided by the core folds of ribosomal proteins. Similar to h18 and h44, rRNA rearrangements in these regions require prior dissociation of assembly factors that stabilize the immature conformation (fig. S15). As a general assembly principle, the immature rRNA of the assemblosome is sandwiched between a preformed shell of ribosomal proteins and a large cluster of assembly factors. Upon departure of the assembly factors, the rRNA is released along with the flexible tails of ribosomal proteins to fold into the cradle formed by the ribosomal proteins (Fig. 5). Afterwards, as seen in the middle and late assembly intermediates, a second cluster of protein factors binds to the rRNA, potentially to protect it from degradation or prevent premature joining of the mitoribosomal subunits.

Outlook

These findings provide evidence for the existence of an intricate machinery for SSU maturation in mitochondria that involves a large number of assembly factors and proceeds through the formation of distinct assembly complexes. Whereas the assembly progression for the three identified intermediates can be inferred from their structure and composition, it remains unclear if these are parts of a linear process or originate from parallel maturation paths. Because several of the assembly factors have homologs in bacteria and in other mitochondria, our results provide general insights for better understanding the bacterial and mitochondrial ribosomal maturation processes.

REFERENCES AND NOTES

1. P. Bieri, B. J. Greber, N. Ban, *Curr. Opin. Struct. Biol.* **49**, 44–53 (2018).
2. D. J. F. Ramrath *et al.*, *Science* **362**, eaau7735 (2018).
3. J. H. Davis, J. R. Williamson, *Philos. Trans. R. Soc. B* **372**, 20160181 (2017).
4. D. Kressler, E. Hurt, J. Baßler, *Trends Biochem. Sci.* **42**, 640–654 (2017).
5. C. Peña, E. Hurt, V. G. Panse, *Nat. Struct. Mol. Biol.* **24**, 689–699 (2017).
6. A. Brown *et al.*, *Nat. Struct. Mol. Biol.* **24**, 866–869 (2017).
7. A. Zíková *et al.*, *Mol. Cell. Proteomics* **7**, 1286–1296 (2008).
8. B. Schimanski, T. N. Nguyen, A. Günzl, *Eukaryot. Cell* **4**, 1942–1950 (2005).
9. D. De Silva, Y. T. Tu, A. Amunts, F. Fontanesi, A. Barrientos, *Cell Cycle* **14**, 2226–2250 (2015).

10. Z. Shajani, M. T. Sykes, J. R. Williamson, *Annu. Rev. Biochem.* **80**, 501–526 (2011).
11. A. M. Mulder *et al.*, *Science* **330**, 673–677 (2010).
12. J. Conrad, L. Niu, K. Rudd, B. G. Lane, J. Ofengand, *RNA* **5**, 751–763 (1999).
13. J. Wrzesinski, A. Bakin, K. Nurse, B. G. Lane, J. Ofengand, *Biochemistry* **34**, 8904–8913 (1995).
14. I. Aphasizheva *et al.*, *Mol. Microbiol.* **99**, 1043–1058 (2016).
15. H. L. Schubert, R. M. Blumenthal, X. Cheng, *Trends Biochem. Sci.* **28**, 329–335 (2003).
16. P. V. Sergiev, N. A. Aleksashin, A. A. Chugunova, Y. S. Polikanov, O. A. Dontsova, *Nat. Chem. Biol.* **14**, 226–235 (2018).
17. J. Týč, L. Novotná, P. Peña-Diaz, D. A. Maslov, J. Lukeš, *Mitochondrion* **34**, 67–74 (2017).
18. C. Saveanu *et al.*, *J. Biol. Chem.* **276**, 15861–15867 (2001).
19. S. Kimura, T. Suzuki, *Nucleic Acids Res.* **38**, 1341–1352 (2010).
20. Y. Wei *et al.*, *J. Struct. Biol.* **179**, 29–40 (2012).
21. M. Pusnik, I. Small, L. K. Read, T. Fabbro, A. Schneider, *Mol. Cell. Biol.* **27**, 6876–6888 (2007).
22. C. Shen *et al.*, *Nat. Commun.* **7**, 11285 (2016).
23. H. Spåhr *et al.*, *Nat. Commun.* **9**, 2212 (2018).
24. S. Holzer, N. Ban, S. Klinge, *J. Mol. Biol.* **425**, 4154–4160 (2013).
25. B. Koch *et al.*, *J. Biol. Chem.* **287**, 21806–21815 (2012).
26. J. G. Van Vranken *et al.*, *Mol. Cell* **71**, 567–580.e4 (2018).
27. A. Leitner *et al.*, Discovery and structure of the mitoribosomal SSU assemblosome in trypanosomes. PRIDE database (2019); doi: 10.6019/PXD011988.

ACKNOWLEDGMENTS

M.S. thanks A. Jomaa and N. C. Schlüter for helpful discussions. A.L. thanks R. Aebersold for access to instrumentation and infrastructure. B. Schimanski is thanked for the 427 single-marker strain. EM data were collected at the Scientific Center for Optical and Electron Microscopy (ScopeM) at ETH Zurich. **Funding:** This work was supported by the Swiss National Science Foundation (SNSF) and the National Center of Competence in Research (NCCR) RNA & Disease Program of the SNSF. D.J.F.R. was supported by a FEBS long-term fellowship. S.M. was supported by an EMBO long-term fellowship (ALTF 793-2017) and by a Human Frontier Science Program long-term fellowship (LT000008/2018-L). **Author contributions:** M.N., S.C., E.K.H., and A.Sch. designed, performed, and interpreted the trypanosome experiments. D.J.F.R., M.N., C.P., M.S., and S.M. purified the SSU-related particles. A.L. performed mass spectrometric analysis. M.S., D.J.F.R., C.P., S.M., A.Sca., P.B., and D.B. collected cryo-EM data. M.S., D.J.F.R., S.M., and A.Sca. calculated the EM maps. M.S., D.J.F.R., C.P., and M.L. built the molecular models. M.S., M.L., and N.B. interpreted the structure. M.S., D.J.F.R., M.N., S.M., M.L., and N.B. drafted the manuscript and figures. D.J.F.R., M.N., C.P., S.C., A.Sca., P.B., A.L., D.B., and A.Sch. edited the manuscript. **Competing interests:** The authors declare no competing interests. **Data and materials availability:** Atomic coordinates have been deposited in the Protein Data Bank (PDB) under the accession codes 6SG9 (head domain), 6SGA (body domain), and 6SGB (complete). The cryo-EM density maps have been uploaded to the Electron Microscopy Data Bank (EMDB) under the accession codes EMD-10175 (affinity-purified mt-SSU assemblosome, head domain), EMD-10177 (affinity-purified mt-SSU assemblosome, body domain), EMD-10180 (affinity-purified mt-SSU assemblosome, complete), EMD-10176 (native mt-SSU assemblosome), EMD-10178 (middle assembly intermediate), and EMD-10179 (late assembly intermediate). Mass spectrometry data have been deposited with the ProteomeXchange Consortium via PRIDE partner repository with the dataset identifiers PXD011988 and 10.6019/PXD011988 (*27*).

SUPPLEMENTARY MATERIALS

science.sciencemag.org/content/365/6458/1144/suppl/DC1
Materials and Methods
Supplementary Text
Figs. S1 to S16
Tables S1 and S2
References (*28*–*51*)
Data S1

4 January 2019; resubmitted 2 July 2019
Accepted 4 August 2019
10.1126/science.aaw5570

Mitoribosomal small subunit biogenesis in trypanosomes involves an extensive assembly machinery

Martin Saurer, David J. F. Ramrath, Moritz Niemann, Salvatore Calderaro, Céline Prange, Simone Mattei, Alain Scaiola, Alexander Leitner, Philipp Bieri, Elke K. Horn, Marc Leibundgut, Daniel Boehringer, André Schneider and Nenad Ban

Science **365** (6458), 1144-1149.
DOI: 10.1126/science.aaw5570

Assembly pathway for mitoribosome

The biogenesis of ribosomes is a multistep process facilitated by assembly factors. Saurer *et al.* provided structural information on the maturation process of the mitochondrial ribosome, or mitoribosome, in the parasitic protozoan *Trypanosoma brucei* (see the Perspective by Karbstein). Cells evolved a dedicated machinery for maturation of the small subunit of the mitoribosome, including the formation of three distinct and well-structured assembly intermediates. Comparison of intermediates and the mature mitoribosome reveals how assembly factors and ribosomal proteins work together to fold and stabilize ribosomal RNA.

Science, this issue p. 1144; see also p. 1077